Disclinations and Their Interactions in Thin Films of Side-Chain Liquid Crystalline Polymers

ARTICLE *in* MACROMOLECULES · JANUARY 2004

Impact Factor: 5.8 · DOI: 10.1021/ma035240o

3 AUTHORS:

Shanju Zhang
California Polytechnic State University, San L…
52 PUBLICATIONS **770** CITATIONS
SEE PROFILE

Eugene M Terentjev
University of Cambridge
304 PUBLICATIONS **7,433** CITATIONS
SEE PROFILE

Athene Donald
University of Cambridge
328 PUBLICATIONS **9,597** CITATIONS
SEE PROFILE

Disclinations and Their Interactions in Thin Films of Side-Chain Liquid Crystalline Polymers

Shanju Zhang, Eugene M. Terentjev, and Athene M. Donald*

Cavendish Laboratory, University of Cambridge, Madingley Road, CB3 0HE, Cambridge, UK

Received August 21, 2003; Revised Manuscript Received October 24, 2003

ABSTRACT: Two-dimensional disclinations formed in thin films of a side-chain liquid crystalline polymer are investigated using transmission electron microscopy (TEM). The detailed director patterns are revealed through nanoscale stripes, which are parallel to the molecular director. One hyperbolic pattern of a negative disclination with a charge $s = -1$ and three patterns involving radial, circular, and spiral director fields of a positive disclination with $s = +1$ are observed. Positive disclination cores are found to exhibit circular dark centers while the $s = -1$ is shown to have a bright central core. The difference in TEM contrast is attributed to the nature of the packing within the core. From the director texture around a disclination it is possible to determine the elastic anisotropy, which is not higher than 0.1. Observing the time evolution of the disclination density, it is found that the average number of defects in the plane scales with time as $N \propto t^{-3/4}$. It is found that both translation and rotation motions occur for a pair of $(+1, -1)$ disclinations, leading to the formation of a certain special configuration shortly before the pair annihilation. In some cases, not the pairs but the linear clusters of three-disclination dominate the interaction. Theoretical analysis is presented to explain this new phenomenon. In addition, director inversion walls are observed to form during the late stage of disclination annihilation. It is found that inversion walls always separate a pair of $(+1, +1)$ disclinations.

Introduction

Liquid crystals (LC) are characterized by a preferred orientational order, which is described by an apolar director **n** field. The most probable director configuration is determined by minimization of the total free energy with respect to the director field. In deformed liquid crystals, disclinations are rotation symmetry-breaking defects. The strength of a disclination corresponds to the number of rotations of the director around a path encircling the disclination.[1] Disclinations and their interactions have been theoretically investigated for many years.[2−5] Such experimental studies are limited in scope in that most of them use optical microscopy to study small molecular LCs or liquid crystalline polymers (LCP's).[4−7] The pairwise interaction of disclinations is analogous to the electrostatic interaction between line charges. The interaction forces are inversely proportional to the distances. Disclinations of opposite sign attract and annihilate each other, while disclinations of the same sign repel each other. This interaction leads to the annihilation of defects and hence a decrease in their number density. The details of these processes are, however, still far from being understood due to both the complexity of potential many-body disclination interactions and the lack of suitable, high-resolution, experimental methods.

Transmission electron microscopy (TEM) is a useful method for studying the microstructure at a molecular level. It has proved to be of great utility in the study of LCP's over the past two decades.[8,9] In the case of semicrystalline LCP's, crystalline lamellae, which are formed perpendicular to the local director, can be used to decorate molecular orientation, and the director trajectories around a disclination are, therefore, directly visualized via TEM.[10,11] This technique to explore the director orientation in semicrystalline LCP's has been successfully applied for the analysis of disclinations and their interactions in main-chain LCP's.[12−14] Hudson and Thomas studied the structure around cores of half-integer disclinations (charge $s = \pm 1/2$) by analysis of the elastic anisotropy.[15] They found that a rigid polymer splayed more at the near-core, while a flexible polymer bent more. Hudson and Thomas also studied disclination ($s = \pm 1/2$) interactions in applied magnetic and extensional flow fields.[16] They observed that a stable four-body disclination cluster (a so-called Lehmann cluster) dominated the interaction at weak and intermediate field strengths. However, almost no observation of director fields of disclinations in side-chain amorphous LCP's systems has been reported to date.[17]

Side-chain LCP's present a unique class of materials with mesomorphic and viscoelastic behavior.[18,19] Their microstructures result from the delicate balance between liquid crystalline order due to the mesogenic core and statistical disorder due to the polymer backbone entropy. In side-chain LCP's, the orientational properties are carried by the short mesogenic side chains, and the nature of the order parameter is then similar to that in small-molecule LC's.[20] In contrast to main-chain systems, there are many theoretical and experimental indications that the values of Frank elastic constants in side-chain LCP's are close to those in analogous small-molecule LC's.[21,22] Therefore, the problems of molecular packing are of a different nature in main-chain and side-chain systems. Recently, we reported the observation of two-dimensional nanoscale stripes in thin films of a side-chain smectic polymer using TEM.[23] When the samples were cooled to the smectic phase, after a holding period in the nematic phase, a characteristic surface morphology developed. This morphology manifested itself in bright field TEM images as a series of nanostripes which aligned along the local director. This orientation was demonstrated by correlating the direction of the stripes with electron diffraction patterns.

* Corresponding author.

10.1021/ma035240o CCC: $27.50
Published on Web 12/18/2003

Stripes resulted from an equilibrium instability, an analogy with the Rayleigh−Taylor instability which in this case occurs due to the competition between the layer-aligning effect of the substrate and the planar director alignment, forcing smectic layers perpendicular to the film surface. We found that the film thickness and annealing temperature affected the stripe width and amplitude while the annealing time only affected the perfection of the stripe alignment—and by implication the perfection of the underlying director pattern. Stripes serve to decorate the underlying molecular alignment, yielding a high-resolution map of director fields over length scales down to tens of nanometers.

In this paper, we extend the stripe-decoration technique to study disclinations and their interactions in side-chain LCP's. We observe the four types of patterns of disclinations with integer charge, $s = \pm 1$, and their inner core structures with their different types of packing are revealed for the first time. By controlling the annealing time in the nematic phase, and hence the average separation of pairs of disclinations, after quenching we observe that each pair of disclinations with opposing sign move together and annihilate via a certain special configuration, as both translational and rotational motions occur. Also, through direct observation of the decorated director field, characteristic linear clusters of three-body disclinations are revealed. To our best knowledge, these results are the first experimental observation showing the details of the annihilation process of disclinations with $s = \pm 1$. We put forward arguments that explain why special configurations of pairs of disclinations occur and why linear clusters of three disclinations form during the late stage of the annihilation process.

Experimental Section

The polymer in this work is an end-on fixed side-group liquid crystalline polysiloxane denoted as SCP-4. The material was kindly prepared for us in house by Dr. A. R. Tajbakhsh. The detailed procedure can be found in the pioneering work of Finkelmann and Rehage.[24] Its chemical structure is

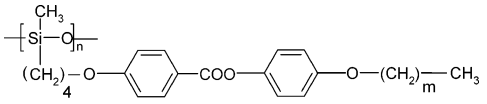

m=4, n=60

Its phase behavior was studied by differential scanning calorimetry (DSC) and polarizing microscopy. The polymer has a glass transition (T_g) at 12 °C, a smectic−nematic transition at 82 °C, and a nematic−isotropic transition at 97 °C. The phases were identified by characteristic textures observed under the polarizing microscope.[23]

Thin films were prepared by the spin-coating method by spinning onto carbon-coated mica from a 1% chloroform solution of the polymer at a speed of 2000−3500 rpm. After complete solvent evaporation, the films were heated to the nematic phase at 90 °C for different times to develop the texture and subsequently quenched to room temperature. The thin films were stripped, floated on the water surface, and collected on copper grids for TEM investigation. The microstructures and morphologies of thin films were observed using a TECNAI-20 TEM at an accelerating voltage of 120 kV. The samples were examined without staining or shadowing under TEM: only a defocusing technique was used to obtain the contrast of the images.[25] The atomic force microscope (AFM) images were obtained using a Nanoscope IIIa scanning probe microscopy (Digital Instruments) operated in tapping mode at ambient conditions. A single-crystal silicon probe tip was used.

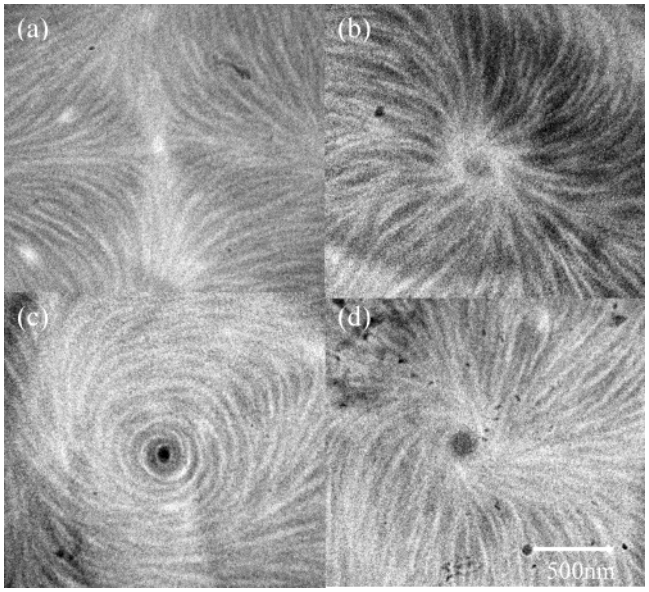

Figure 1. A series of TEM micrographs of the different types of integral disclinations: (a) hyperbolic pattern (H), $s = -1$; (b) radial pattern (R), $s = +1$, $c = 0$; (c) circular pattern (C), $s = +1$, $c = \pi/2$; (d) spiral pattern (S), $s = +1$, $0 < c < \pi/2$. At late stages of annealing when the disclination density is low, stripes can reveal different patterns of disclinations with $s = \pm 1$ in isolation.

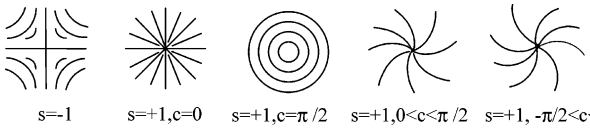

Figure 2. Schematic diagram of molecular trajectories in a two-dimensional ordered liquid crystal associated with disclinations of $s = \pm 1$, predicted by Frank continuum theory.

Images of each sample were recorded in height and phase contrast modes and analyzed with the Nanoscope image processing software.

Results and Discussion

Isolated Disclinations. Figure 1 shows the four typical morphologies and structures around disclinations in isolation (far from any neighbor or sample boundary). As the director lies parallel to the local alignment of the stripes, the orientation of stripes reveals real trajectories of the directors around a disclination.[23] One can immediately notice the pattern of contrasting stripes which evidently decorate the disclinations of strengths $s = \pm 1$. We found only one type of disclination with strength $s = -1$. This has a hyperbolic structure (H) with 4-fold symmetry (Figure 1a), while disclinations with strength $s = +1$ have three different types of director structure: radial (R), circular (C), and spiral patterns (S) (Figure 1b−d). These patterns are distinguished by a value of constant parameter c, which relates the axial position in the plane around the disclination core (polar angle θ) and the director orientation angle: in the simplest case $\phi(\theta) = s\theta + c$, as described by Frank in his continuum theory.[1] According to this theory, one negative pattern and three positive patterns can be expected in a two-dimensional ordered liquid crystal, as shown in Figure 2. Radial and circle patterns occur when the constant c is 0 and $\pi/2$, respectively. For other values of c from $-\pi/2$ to $\pi/2$, spiral patterns occur, which may have either sense (right- or left-handed). The energies of spiral patterns

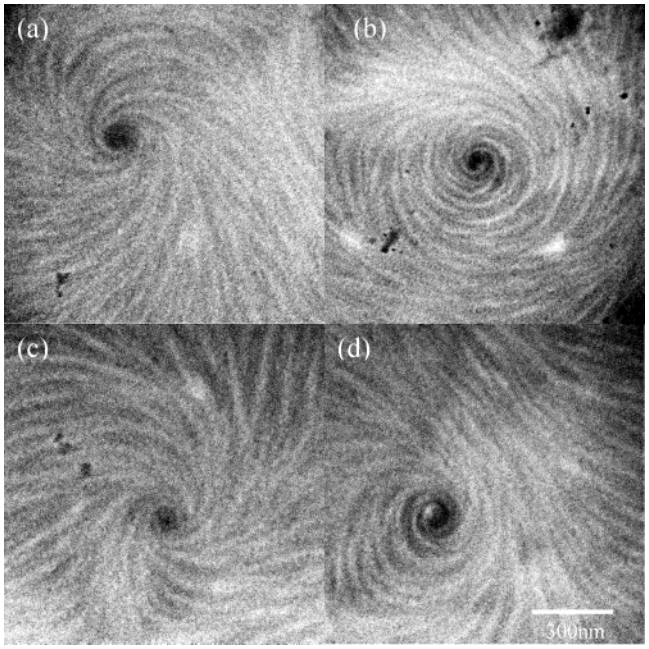

Figure 3. A set of TEM micrographs of spiral patterns showing different configurations: (a) left-handed with $c = -\pi/6$; (b) left-handed with $c = -\pi/3$; (c) right-handed with $c = \pi/6$; (d) right-handed with $c = \pi/3$. The energy of all these configurations is the same. The different value c is determined by the ratio of bend and splay distortions.

with different c values are identical according to Frank, and hence the numbers of left-handed and right-handed spirals should be equal. This is observed in our experiments. We captured hundreds of images and found that the numbers of left-handed and right-handed spirals were approximately equal. Figure 3 shows a series of spiral structures, both left-handed and right-handed and with different values of the constant c. The greater the absolute value of c, the more bend distortion is stored in the director field. For any given material, only radial or circular patterns of a positive disclination should be stable, according to whether the bend or splay elastic constant is larger.[1] That all the different configurations of disclinations with $s = \pm 1$ were observed in this study indicates that the splay and bend elastic constants in our SCLCP must be of the same order of magnitude. This is in agreement with previous elastic constants measurement of side-chain liquid crystalline polymers.[21,22]

In the two-dimensional thin film geometry applicable here (in which twist distortions can be ignored), the elastic anisotropy for splay and bend distortions can be defined in terms of the parameter ϵ defined by

$$\epsilon = (k_{11} - k_{33})/(k_{11} + k_{33}) \qquad (1)$$

where k_{11} is the splay and k_{33} the bend elastic constant. For an isolated disclination, the director field is described by the local director orientation ϕ at a polar angle θ, defined relative to a reference axis. The function $\phi(\theta)$ depends only on the relative splay and bend elastic anisotropy. For small values of ϵ, the first-order perturbation expansion of the director orientation in terms of ϵ is given as[15]

$$\phi(\theta) = s(\theta + \theta_0) + \epsilon[s(2 - s)/4(s - 1)^2] \sin[2(s - 1)(\theta - \theta_0)] \qquad (2)$$

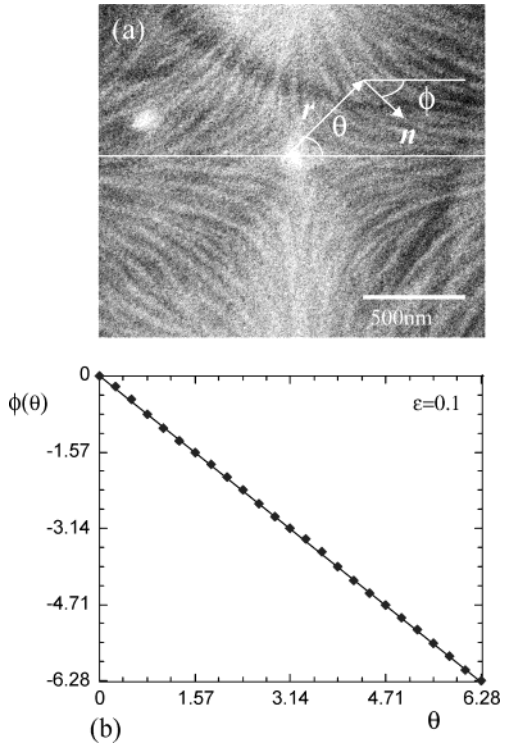

Figure 4. (a) Electron micrograph of the SCP-4 polymer showing an $s = -1$ disclination used for measuring the elastic anisotropy ϵ. Scale bar is 500 nm. (b) Data for $\phi(\theta)$ taken from (a) at a radius of 0.8 μm from the disclination center. Solid line through the data is the fit obtained by varying ϵ.

where s is the topological disclination strength and θ_0 is the orientation of the disclination. (The full solution for disclinations at arbitrary Frank elastic anisotropy[27] is more complicated and unnecessary for our case of small ϵ; however, this may not be the case in main-chain LCP's with $k_{11} \gg k_{33}$.) As it is possible to image the director field at high resolution, we can determine $\phi(\theta)$ and hence the anisotropy parameter ϵ, following the method originally developed by Hudson and Thomas.[15,26] Figure 4a is a TEM micrograph of an $s = -1$ disclination in the SCP-4 sample. The director field orientation $\phi(\theta)$, at radius r from the core, can be obtained from the director field as revealed by the stripes. The origin is defined once the core position of the disclination has been identified. Figure 4b shows the data $\phi(\theta)$ collected from Figure 4a at a radius of 0.8 μm. The elastic anisotropy is determined by a least-squares fit of the theory to the data. To reduce the measurement error, we selected several isolated disclinations (so that they were substantially unaffected by their neighbors) and for different radius values for a single disclination. Measurements yield a good fit to the theory expressed by eq 2 with ϵ not higher than 0.1, which produces k_{11}/k_{33} not higher than 1.2. Thus, our results show that the splay and bend elastic constants in this side-chain liquid crystalline polymer are of the same order of magnitude, just as found in small molecular liquid crystals, but in contrast to main-chain liquid crystalline polymers.

It is interesting to note that our stripe-decoration technique can also reveal the inner core structure of the disclination. In TEM bright-field images, as shown in Figure 1, the positive disclinations with $s = +1$ including radial, circular, and spiral patterns have circular dark regions at their core, while the hyperbolic pattern of the negative disclination with $s = -1$ exhibits a bright

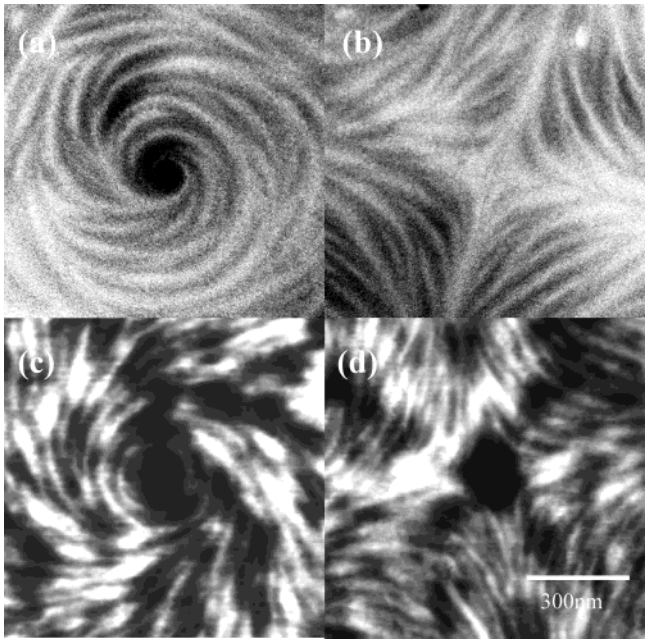

Figure 5. Comparison of core structures between +1 and −1 disclinations as viewed in TEM and AFM images: (a) and (c) spiral patterns of $s = +1$ disclination; (b) and (d) hyperbolic patterns of $s = -1$ disclination. Different contrast in AFM height images of (c) and (d) reflects thickness undulations and thin regions correspond to dark ones. The vertical scale is 5 nm.

central region. However, in AFM height-contrast images, the core in all the patterns of the integral disclinations shows a dark center, indicating the local depression in the film thickness. Comparison between positive and negative disclination cores for both TEM images and AFM height images is shown in Figure 5. In our previous work, we argued that any dark regions in the TEM bright field image could result from two possible sources of the contrast: the director orientation moving out of the film plane and thickness variations in the polymer film.[23] Here we can exclude thickness as the source of contrast for the inner core because of the results from the AFM height images. Both positive and negative disclination cores are seen to be thinner than the surrounding material. This would be consistent with the idea of mesogenic groups tilting out of the plane of the film within the core, for both types of disclinations.[28] For the $s = +1$ case, diffraction contrast due to the mesogen orientation appears to dominate in the TEM image, leading to the central region looking dark. Conversely, for the $s = -1$ disclination, the thinning of the material within the core dominates leading to its bright appearance, presumably either because the tilt of the molecules is less in this case or the packing is less ordered. That the molecules in both positive and negative disclination cores tend to align perpendicular to the surface agrees well with the theoretical predictions of "escape into the third dimension".[5] Further details about the theoretical analysis of the core structure will be published in a separate paper.

Interaction of Disclinations. To study disclination interactions, different annealing times have been employed to alter disclination separations. Figure 6 shows changes in the stripe alignment in thin films annealed at 90 °C for different times. Initially, the stripes are not well aligned, and decorate many defects, as shown in Figure 6a. With an increase of the annealing time, defects tend to annihilate one other, and stripes reveal

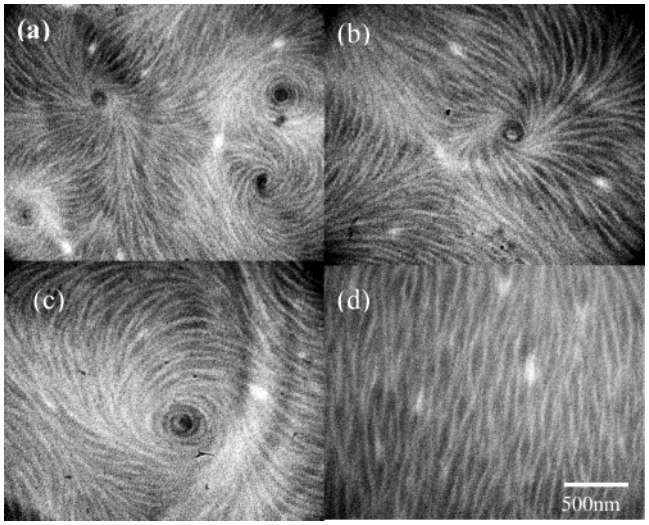

Figure 6. A set of TEM micrographs of thin films of SCP-4 annealed at 90 °C for different times: (a) 30, (b) 60, (c) 120, and (d) 1440 min. With an increase of annealing time, the degree of alignment of the stripes change but without changes in width or amplitude.

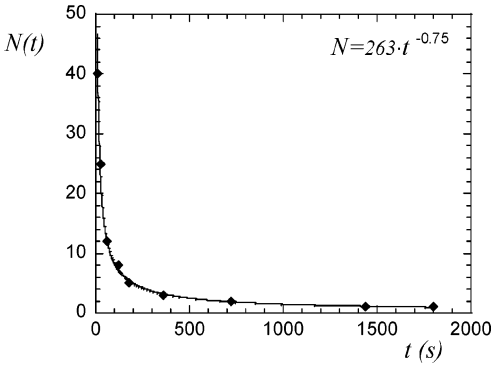

Figure 7. Evolution of number density of defects for an area of $10 \times 10\ \mu m^2$ following annealing thin films at 90 °C (from the AFM data). The solid line is a power-law fit with an exponent of $^3/_4$.

a more uniform director orientation. Parts b and c of Figure 6 show a pair of disclinations and an isolated disclination, respectively. When the film is left to equilibrate for a long time, the stripes demonstrate the presence of large defect-free regions basically spanning the film. The resulting parallel structure exhibits a high degree of anisotropy, as shown in Figure 6d.

Theoretically, the defect density is predicted to scale with time t as t^{-y}, where the exponent depends on details of the order parameter and the spatial dimensionality.[29−32] We counted the average number of disclinations in a given area as a function of annealing time at 90 °C. In Figure 7, the average number (N) of defects per area of $10 \times 10\ \mu m^2$ is plotted against the annealing time t (min). The data points fall onto a line obeying the scaling relationship of $N \propto t^{-3/4}$. Accordingly, the average spacing between adjacent disclinations in the plane is scaled as $N^{-1/2} \propto t^{3/8}$. Thus, by controlling the annealing time for the thin films to make the distance between adjacent disclinations large enough that properties of isolated disclinations and pairs thereof can be studied, we can investigate the interactions.

Interactions between several disclinations are very complex. Studies on simple cluster interactions, such as a pair, three-body, or four-body coupling, can help us understand such a complex system. As mentioned

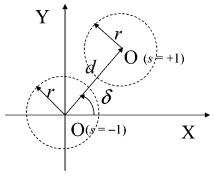

Figure 8. Schematic diagram of a pair of (+1, −1) disclinations. The core of a −1 disclination is the origin with its symmetric axis fixed along the *X* axis. The distance between two disclinations is defined by *d*. The angle δ is the angle between the line joining the two cores and *X*-axis direction. The relative orientation and position of the disclinations are determined by parameters of *d* and δ.

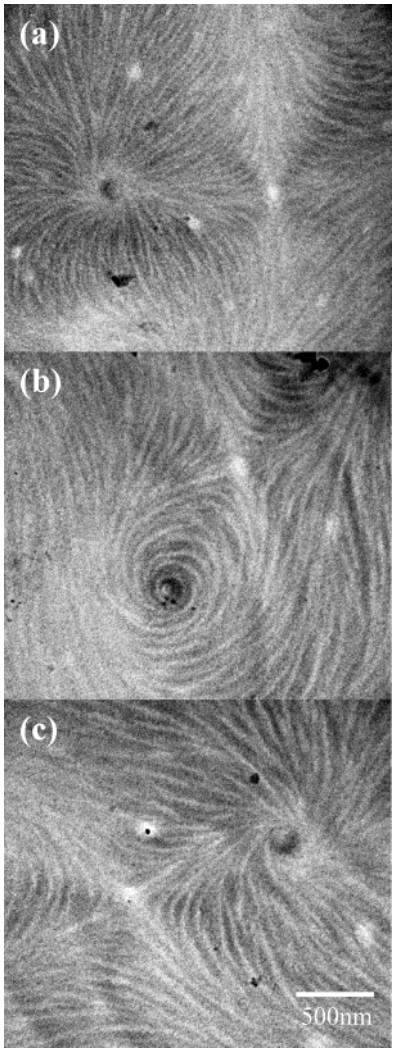

Figure 9. A set of TEM micrographs of three typical configurations of (+1, −1) disclinations: (a) radial−hyperbolic (R, H), $\delta = 0$; (b) circular−hyperbolic (C, H), $\delta = \pi/4$; (c) spiral−hyperbolic (S, H), $0 < \delta < \pi/4$. One can see that the director rotates continuously in space.

above, with an increase in annealing time, defect densities decrease. Thus, the distance between two adjacent disclinations becomes large enough to study their interactions.

Imagine that a $s = +1$ disclination is positioned at some point near a $s = -1$ disclination, as shown in Figure 8. A coordinate frame is chosen such that the core of the −1 disclination is taken as the origin, and one of its symmetric axes is taken as the *X*-axis. For this study we choose to take one of the lines for which the director is radial (either the vertical or horizontal

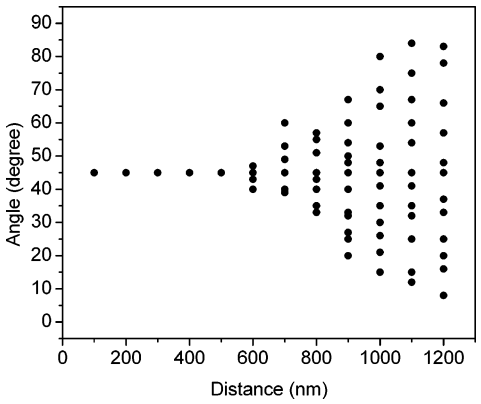

Figure 10. A plot of the angle δ vs the distance *d* between two disclinations of hyperbolic and circular types. The parameters δ and *d* are defined in Figure 8.

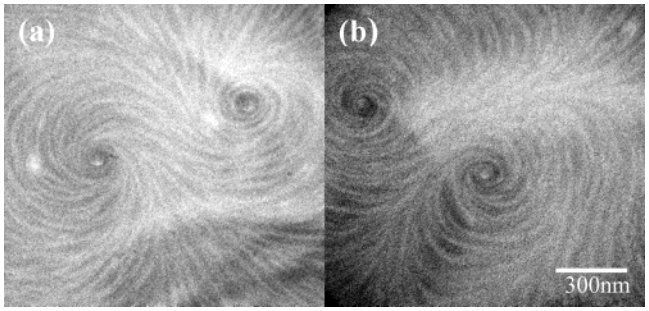

Figure 11. A set of TEM micrographs of typical configurations of spiral−spiral (S, S) disclinations: (a) equal-handed spirals; (b) opposite-handed spirals. Inversion walls always terminate the (S, S) disclinations. During the annihilation, positive disclinations separate each other due to the repelling force.

axis for the geometry shown in Figure 1). The angle between the line joining the two disclination cores and the *X* axis is called δ, and the distance between the two disclinations is called *d*. The relative orientation and separation of the two disclinations are therefore completely determined by the parameters of δ and *d*. Figure 9 shows three typical configurations of (+1, −1) pairs of disclinations after relatively long annealing times. For a pair of radial (R) and hyperbolic (H) disclinations, denoted as (R, H), the R core lies on a symmetry axis of H. The line joining R and H cores is therefore parallel to the *X* axis, and the angle δ is hence 0. For a pair of circular (C) and hyperbolic (H) disclinations, denoted as (C, H), the angle δ is $\pi/4$. For a pair of spiral (S) and hyperbolic (H) disclinations, denoted as (S, H), the angle δ lies between 0 and $\pi/4$. Recalling that *c* is a variable for S disclinations, reflecting the balance between splay and bend distortions, it is clear that the value of δ will also depend on the particular value of *c*. The larger the ratio of splay to bend, the larger the angle δ is. The energy of all these configurations is the same in the one-constant approximation of Frank elasticity. Special geometrical shapes of positive disclinations determine the different configurations. These experimental results agree well with the theoretical prediction.[2]

In the early stages of annealing, before the attraction of disclinations of opposite signs has brought pairs together, the distance *d* is large and various configurations with different angles δ for each of (R, H), (C, H), and (S, H) pairs are observed. When the distance *d* is below a critical value, only one configuration with a constant angle δ is observed for each pair (as shown

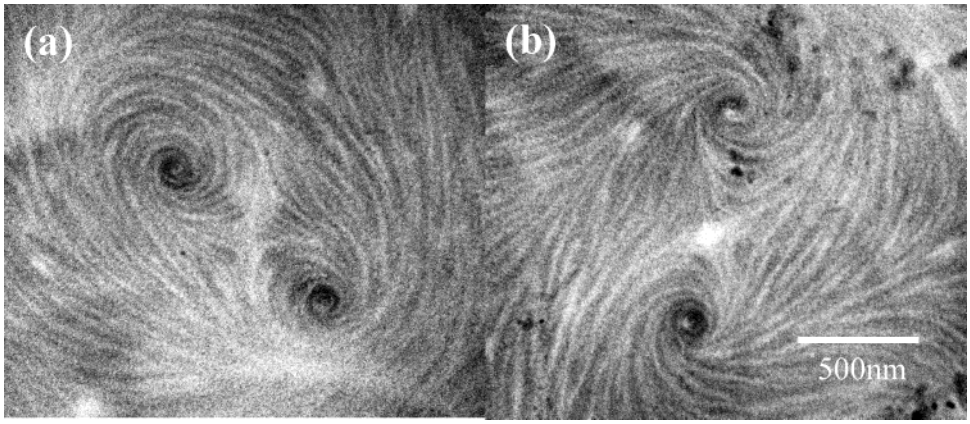

Figure 12. A set of TEM micrographs of typical configurations of three-body clusters formed at a late stage of the annihilation process: (a) circular−hyperbolic−circular (C−H−C); (b) spiral−hyperbolic−spiral (S−H−S). Three disclinations aggregate together and form linear clusters in isolation. The different configurations of linear clusters for three-body disclinations are determined by the energetics of the system plus geometrical constraints. After the end of the annihilation, a new disclination should form to balance the topological charge of the system.

above). This critical value means that at this distance the energetics of interaction lead to a special geometrical relationship between the pair of disclinations. Figure 10 shows how the orientation between pairs of disclinations (C, H) changes as a function of the distance d. At early annealing times, when d is large, the angle δ varies between 0 and $\pi/2$. However, as the annealing time increases and the disclinations attract each other so that d decreases, the angle δ has a tendency to move toward the single value of $\pi/4$. When the distance d reaches the critical value of $d \sim 500$ nm, the angle δ is always $\pi/4$ for all disclination pairs. Below this critical value, the angle of $\pi/4$ is maintained until the end of the annihilation process. Reduction in d implies translation of the disclination(s), and the change of angle δ must require rotational motion. Thus, the annihilation process involves both types of motion. In other words, both radial and angular forces drive annihilation at early times, when $d > 500$ nm. At late times, once $d < 500$ nm, only the radial force must be operative once the equilibrium value of δ has been achieved.

In addition to pairs of disclinations of opposite sign, we also observed pairs of disclinations of the same sign. Figure 11 shows typical configurations of (S, S) pairs with opposite and similar handedness. The inversion walls (see below) terminating a pair of spiral patterns were observed. At an early stage, the distance between S−S cores is small. Because of the repulsive force between disclinations of the same sign, the disclinations move apart and d increases. Finally, each positive disclination may move near a negative one and form a new pair of (+1, −1) disclinations as discussed above.

It is interesting to note that in some cases we observed characteristic linear clusters of three-body disclinations in isolation at a late stage of the annihilation. Figure 12 shows two typical kinds of such clusters of circular−hyperbolic−circular (C−H−C) and spiral−hyperbolic−spiral (S−H−S). One can see that disclinations in all these clusters are collinear. A linear cluster has a lower energy than an angular cluster because the interaction of opposite-signed disclinations is strongly attractive. Once a linear cluster forms, the same-signed disclinations are most shielded from each other and both are attracted to the central, opposite signed disclination at the center of the cluster. Thereafter, the cluster can shrink slowly without change of type or symmetry. After annihilation, a new disclination must form to balance the topological charge of the system. Thus, we would expect that a new $s = +1$ disclination forms after the decay of (C−H−C) or (S−H−S) cluster.

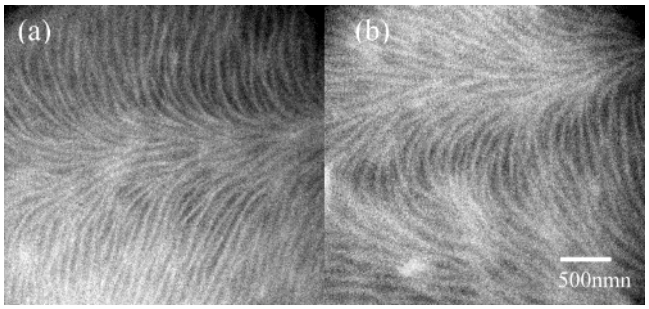

Figure 13. TEM micrographs of inversion walls: (a) splay wall; (b) bend wall. Inversion walls form with long-time thermal treatment and connect the disclinations. A splay wall has primarily splay distortion while a bend wall has primarily bend distortion.

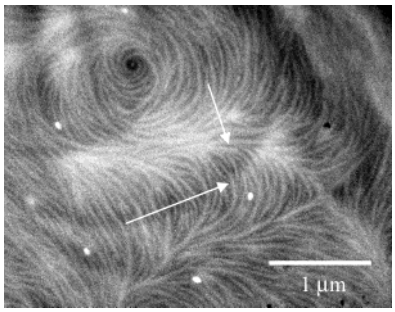

Figure 14. TEM micrographs of inversion walls terminating the disclinations. Splay and bend walls (indicated by arrows) separate a pair of $s = \pm 1$ disclinations. Note that distortions are introduced in the disclination texture.

Other Defects. Other than disclinations of integer strength, an isolated inversion wall can also be observed in our LCP films. Figure 13 shows two kinds of inversion walls: splay and bend walls, according to the main mode of curvature elasticity of director distortions. Inversion walls have mirror symmetry and lead to a discontinuous change in the molecular director across the wall. The director undergoes a rotation of π from one side of the wall to the other. We found that inversion walls formed during the late stage of the annihilation process of defects and connected pairs of remaining disclinations. Figure 14 shows the inversion walls (splay and bend)

connecting a pair of ±1 disclinations. Note that distortions are introduced as a result of the influence of the walls. The observed stripe-decorated walls observed here are analogous to those in ordinary nematic liquid crystals during the director reorientation via flow, electric, or magnetic fields.[16,33,34]

Conclusion

Two-dimensional nanostripes have been observed in bright field TEM images of thin films of a side-chain liquid crystalline polymer, decorating the local director patterns. Mesogenic molecules in thin films lie nearly homogeneously in the film plane and the nematic director is aligned parallel to the stripe direction. With increase of annealing time, the stripes improve their alignment without change of width or amplitude. By controlling the annealing time, we have studied disclinations of strength $s = \pm 1$ and their interactions at high resolution. One pattern of $s = -1$ (hyperbolic) disclination and three patterns (radial, circular, and spiral) of $s = +1$ disclinations are observed, in good agreement with Frank's theoretical prediction. Handed spiral structures with different ratios of bend and splay distortions are also observed. By analyzing the director fields about isolated disclinations, the elastic anisotropy parameter ϵ is deduced to have a value not higher than 0.1; that is, the bend and splay elastic constants in side-chain liquid crystalline polymers are of the same order. At the core of disclinations, the mesogenic groups have a tendency to align perpendicular to the surface. After long annealing time, inversion walls are commonly observed separating two disclinations.

Disclination interactions (in the absence of any external aligning field) have been investigated via the stripe decoration technique. At early times in the annihilation of (+1,−1) disclination pairs, both translation and rotation control the configuration, which must be determined by radial and angular attracting forces, respectively. At late stages, we have observed specific configurations for each pair of (+1,−1) disclinations. When the disclination separation is <500 nm, only translation motion occurs until the end of the annihilation process. We observe that inversion walls always separate a pair of (+1,+1) disclinations. In some cases, we observe that interactions of pairs of disclinations no longer dominate, but three-body disclinations clusters form. The cluster is always collinear.

Acknowledgment. We thank Dr. Ali Tajbakhsh for kindly providing the polymers. The support of EPSRC is greatly appreciated.

References and Notes

(1) Frank, F. C. *Discuss. Faraday Soc.* **1958**, *25*, 19.
(2) Ranganath, G. S. *Mol. Cryst. Liq. Cryst.* **1983**, *97*, 77.
(3) Liu, C.; Muthukumar, M. *J. Chem. Phys.* **1997**, *106*, 7822.
(4) Chuang, I.; Yurke, B.; Pargellis, A. N. *Phys. Rev. E* **1993**, *47*, 3343.
(5) Nehring, J.; Saupe, A. *J. Chem. Soc., Faraday Trans. 2* **1972**, *68*, 1.
(6) Wang, W.; Leiser, G.; Wegner, G. *Liq. Cryst.* **1993**, *15*, 1.
(7) Cheng, S. X.; Chung, T. S. *J. Phys. Chem. B* **1999**, *103*, 4923.
(8) Donald, A. M.; Windle, A. H. *Colloid Polym. Sci.* **1983**, *261*, 793.
(9) Donald, A. M.; Windle, A. H. *Polymer* **1984**, *25*, 1235.
(10) Wood, B. A.; Thomas, E. L. *Nature (London)* **1986**, *324*, 656.
(11) Thomas, E. L.; Wood, B. A. *Faraday Discuss. Chem. Soc.* **1985**, *79*, 229.
(12) Chen, S.; Cai, L.; Wu, Y.; Jin, Y.; Zhang, S.; Qin, Z.; Song, W.; Qian, R. *Liq. Cryst.* **1993**, *13*, 365.
(13) Shiwaku, T.; Nakai, A.; Hasegawa, H.; Hashimoto, T. *Macromolecules* **1990**, *23*, 1590.
(14) Xie, F.; Hu, Z.; Liu, J.; Yan, D.; He, T.; Wang, B.; Zheng, R.; Cheng, S. Z. D.; Percec, V. *Macromol. Rapid Commun.* **2001**, *22*, 396.
(15) Hudson, S. D.; Fleming, J. W.; Gholz, E.; Thomas, E. L. *Macromolecules* **1993**, *26*, 1270.
(16) Hudson, S. D.; Thomas, E. L. *Phys. Rev. A* **1991**, *44*, 8128.
(17) Ostrovskii, B. I.; Sentenac, D.; Samoilenko, I. I.; De Jeu, W. H. *Eur. Phys. J. E* **2001**, *6*, 287.
(18) Donald, A. M.; Windle, A. H. *Liquid Crystalline Polymers;* Cambridge University Press: Cambridge, 1992.
(19) Shibaev, V. P.; Lam, L. *Liquid Crystalline and Mesomorphic Polymers*; Springer: New York, 1994.
(20) Kleman, M. *Faraday Discuss. Chem. Soc.* **1985**, *79*, 215.
(21) Fabre, P.; Casagrande, C.; Veyssie, M.; Finkelman, H. *Phys. Rev. Lett.* **1984**, *53*, 993.
(22) Schmidtke, J.; Stille, W.; Strobl, G. *Macromolecules* **2000**, *33*, 2922.
(23) Zhang, S. J.; Terentjev, E. M.; Donald, A. M. *Eur. Phys. J. E* **2003**, *11*, 367.
(24) Finkelmann, H.; Rehage, G. *Adv. Polym. Sci.* **1984**, *60*, 97.
(25) Handlin, D. L., Jr.; Thomas, E. L. *Macromolecules* **1983**, *16*, 1514.
(26) Hudson, S. D.; Thomas, E. L. *Phys. Rev. Lett.* **1989**, *62*, 1993.
(27) Anisimov, S. I.; Dzyaloshinskii, I. E. *Sov. Phys. JETP* **1972**, *36*, 774.
(28) Mazelet, G.; Kleman, M. *Polymer* **1986**, *27*, 714.
(29) Toyoki, H. *Phys. Rev. A* **1990**, *42*, 991.
(30) Hashimoto, T.; Nakai, A.; Shiwaku, T.; Hasegawa, H.; Rojstaczer, S.; Stein, R. S. *Macromolecules* **1989**, *22*, 422.
(31) Harrison, C.; Cheng, Z. D.; Sethuraman, S.; Huse, D. A.; Chaikin, P. M.; Vega, D. A.; Sebastian, J. M.; Register, R. A.; Adamson, D. H. *Phys. Rev. E* **2002**, *66*, 011706.
(32) Rieger, J. *Macromolecules* **1990**, *23*, 1545.
(33) Ding, D. K.; Jin, B. Y.; Gunther, J. Thomas, E. L. *Philos. Mag. B.* **1997**, *76*, 951.
(34) O'Rourke, M. J.; Ding, D. K.; Thomas, E. L.; Percec, V. *Macromolecules* **2001**, *34*, 6658.

MA035240O